2014-32-0062
20149062
Published 11/11/2014

doi:10.4271/2014-32-0062
saeeng.saejournals.org

An Analytical Model of a Two-Phase Jet with Application to Fuel Sprays in Internal Combustion Engines

Jonathan Tenenbaum, Michael Shapiro, and Leonid Tartakovsky
Technion Israel Inst. of Technology

ABSTRACT

The paper presents an analytical two-dimensional model of two-phase turbulent jets with focus on fuel sprays in internal combustion engines. The developed model allows prediction of the fuel spray parameters including local fuel concentration and mixture velocity.

The model proposed in this paper is based on the single-phase steady-state laminar axisymmetric jet flow field solution by Schlichting. This solution is amended to include transport of the discontinuous fuel phase in a stagnant air in the limit of a dilute fuel concentration. This two-phase jet flow model admits a closed form analytical solution for the fuel concentration distribution. This solution is then applied to turbulent jet flow as per the approach described by Schlichting and in other studies, and used to predict point-wise properties of fuel sprays in internal combustion engines.

The results of model simulations are compared with the available experimental data. It was found that the analytical model predicts satisfactorily spray properties without additional assumptions or fitting coefficient.

The advantage of the developed model is in its simplicity and rigor in comparison with empirical and numerical models.

CITATION: Tenenbaum, J., Shapiro, M., and Tartakovsky, L., "An Analytical Model of a Two-phase Jet with Application to Fuel Sprays in Internal Combustion Engines," *SAE Int. J. Engines* 8(1):2015, doi:10.4271/2014-32-0062.

INTRODUCTION

Increasingly stringent demands and regulations imposed on engine emissions and efficiency pose challenges for diesel engine manufacturers. To meet these demands engine developers perform computer-aided optimizations to improve the mixture formation and combustion processes, which usually rely on predictions of various physical processes of mixture formation and combustion in the engine [1]. Knowledge of the temporal and spatial behavior of fuel sprays is critical for prediction of engine performance and improvement of its design. Despite the great effort spent on fuel spray modeling, complex phenomena that take place at short time and length scales in diesel fuel sprays make spray modeling a difficult task.

Increasing computing power brings a growing use in computational fluid dynamics (CFD) models, which are a helpful tool in analyzing engine performance. Sprays in such CFD codes are widely modeled by Lagrangian-drop and Eulerian-Fluid method (LDEF) with some models adopting the Eulerian-liquid-Eulerian-gas (two-fluid) method [2]. In the LDEF method spray is divided into parcels containing a predefined mass of fuel that move within the gas-phase grid. The properties of the parcels are coupled with those of the gaseous phase at every time step via mass, momentum and energy transfer between the phases. In the two-fluid method, no additional cells are used and the fuel mass is added to the air contained in the grid [1]. Both methods allow calculation of local and general spray properties in combustion chambers of internal combustion engines.

The accuracy of CFD models strongly depends on mesh selection. A CFD model poorly predicts even general (integral) properties of spray structures when a coarse CFD mesh is used [2, 3, 4]. Normally in these models the mesh sizes is chosen to decrease near the nozzle down to nozzle size resolution. Notwithstanding the results are sensitive with respect to the mesh size choice and still pose problems for engine designers, particularly if the engine size is either too small or too large for using conventional grid sizes [2].

To reduce numerical grid dependency in CFD models, different spray models have recently been developed [4, 5, 6, 7] which do not rely on CFD calculations but rather on analytical or empirical correlations. Some of these models combine CFD calculation of several spray properties with determination of the remaining properties from correlations. Such is the LDEF model of Abani et al. [2], where the drag force between gas

and fuel is calculated from the axial component of the ambient gas velocity derived from the gas jet theory rather than calculated in every time step. This approach is reported to significantly reduce numerical grid dependency in CFD models.

In other LDEF models properties of spray parcels are implied mostly from predictions of analytical or empirical studies of macroscopic spray properties [4], [6]. These models offer an advantage of reduced grid size sensitivity. Another advantage is usage of smaller computing resources (power or time) compared to the CFD models. Even with the available computing power nowadays, the above advantage is important in optimizations of injection parameters, where the spray flow models are used for calculations at various operating conditions. Therefore, analytical and empirical studies of spray properties, and the related models of spray behavior may contribute to the capability of CFD models to predict engine performance and perform optimizations. In this respect analytical fuel spray models, being a versatile tool requiring negligible computational resources, are always preferable.

In the empirical LDEF models, the local dynamic properties of sprays, namely parcel velocity components and fuel concentration within the parcel, are calculated using two macroscopic spray characteristics: spray tip penetration and spray dispersion angle [4], [6]. Using these two properties, an array of parcels traveling within the gas-phase grid can be defined. Axial distributions of velocity and fuel concentration are determined either by analytical or empirical correlations, or by using 1D equations of conservation of mass and momentum [4], [6]. The radial distributions of velocity and fuel concentration are assumed to be characterized by a constant spray dispersion angle [4], [6] or having Gaussian shape [5]. The radial distribution determines the ratio of velocity and fuel concentration between adjacent cells. This approach offers a method of simulation of a transient spray based on empirical correlations with little computing effort and grid size insensitivity. However it is important to notice that radial distributions of mixture velocity and fuel concentration are calculated using two approximations. Namely (i) the spray dispersion angle is calculated using empirical constants, and (ii) the distributions are then assumed to be certain functions of this angle.

Correlations for fuel spray penetration S [6, 7, 8, 9, 10, 11, 12, 13, 14] were obtained either analytically or empirically, being heavily based on the results of experiments. Several analytical studies considered spray as a two-phased jet with predetermined velocity distribution [11], [14], such as the work of Wakuri et al., with the resulting correlation for spray penetration:

$$S = \left(\frac{2C_c \Delta p}{\rho_a} \right)^{0.25} \left(\frac{2tr_i}{\tan\left(\frac{\theta}{2}\right)} \right)^{0.5} \quad (1)$$

where t is the time variable, Δp, ρ_a, are the inlet pressure drop and the gas density respectively, r_i is the inlet jet radius, and θ is the spray dispersion angle, C_c is the coefficient of contraction, defined below.

Hiroyasu and Arai [9] obtained S by solving the equations of conservation of momentum in the spray under the assumption of Levich's break-up length of high velocity liquid jets in the spray, which resulted in the correlation:

$$S = 2.95 \left(\frac{\Delta p}{\rho_a} \right)^{0.25} \left(2tr_i \right)^{0.5} \quad (2)$$

Other correlations either analytical or empirical [10] also obey the relation:

$$S \propto \left(\frac{\Delta p}{\rho_a} \right)^{0.25} \left(tr_i \right)^{0.5} \quad (3)$$

Correlations for spray dispersion angle obtained in several studies [15], [16], [9], [11] vary greatly in their functional forms. Some were obtained from experiments [16], whereas other hinge on fuel mass conservation equations appearing in one-dimensional spray models, such as Hiroyasu and Arai [9] and Wakuri et al. [11]. Naber & Siebers [10] proposed a correlation for θ by examining experimental data collected for various operating conditions of spray penetration.
Correlations for cross-sectionally averaged fuel concentration $\overline{C_f}$ were obtained on either conservation of fuel mass in one-dimensional spray models, Wakuri et al. [11], resulting in the formula:

$$\overline{C_f} = \frac{\sqrt{C_c \rho_f \rho_a} r_i}{x \tan\left(\frac{\theta}{2}\right)} \quad (4)$$

where ρ_f is the fuel drop material density. In contrast, other correlations [6], [4] in which the spray is regarded as an array of parcels were obtained by conservation of momentum in sprays, with incorporating correlations of spray penetration to determine the local mixture velocity in the spray. The correlation of Wakuri et al. was compared with the experimental data of Kamimoto et al. [17], which will also serve as a basis for validation of the present model in this paper.

Experimental correlations also exist for the radial distributions of mixture velocity and fuel concentration. Commonly [14], [18] a Gaussian profile is assumed for both the velocity and fuel concentration:

$$u_x(x,r) = u_x(x,0)\exp\left(-\lambda\left(\frac{r}{x\tan(\theta/2)}\right)^2\right)$$

$$C(x,r) = C(x,0)\exp\left(-\lambda Sc\left(\frac{r}{x\tan(\theta/2)}\right)^2\right) \quad (5)$$

Where *x, r* are the axial and radial coordinates within the jet, *Sc* is the droplets' Schmidt number (see definition below) and a constant λ was determined experimentally.

It can be seen that in order to calculate the radial distribution of velocity and fuel concentration from equation (5) the spray dispersion angle must be measured or correlated. These correlations of radial distributions were validated with experiments in the above mentioned works

It may therefore be seen that existing empirical correlations enable calculation of integral and averaged spray properties. However, no existing correlation allows calculation of local spray properties, in particular local fuel concentration and local mixture velocity within the spray. In other words, in order to calculate local spray properties with existing analytical or empirical correlations, one must rely on either measurements or correlations of the spray dispersion angle, as well as choosing values for constants and assuming functional dependence of several spray quantities.

The goal of this study is to develop an analytical model of two-phase turbulent jets capable of predicting local spray properties without the need for additional correlations of general spray properties. We develop an analytical model for spatial distribution of mixture velocity and drop concentration in fuel sprays and compare the results with the available experimental data.

DEVELOPMENT OF THE MODEL

Physical Model and Assumptions

We consider fuel injected in the combustion chamber as a two-phase axisymmetric circular jet, flowing into an effectively semi-infinite gas space, as schematically depicted in Figure 1.

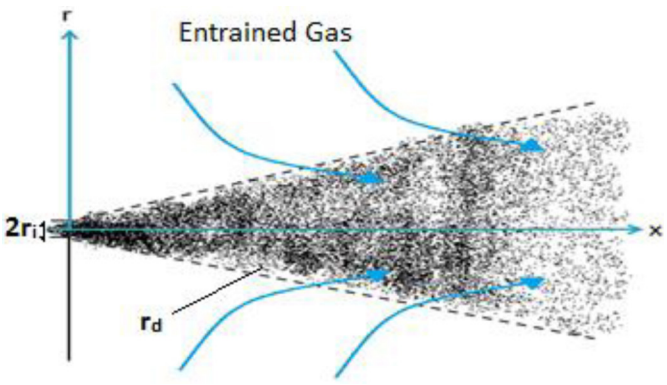

Figure 1. A schematic of the physical model of the fuel jet flow

The jet inlet is assumed to have point size. This implies that the model will be valid for axial distances far exceeding the nozzle inlet diameter. It is assumed also that the spray consists only of fuel droplets suspended in a gas, as the conditions of fuel injection in internal combustion engines correspond to the atomization break-up regime [19]. As such, the jet disintegrates into droplets at a very short distance from the nozzle. The droplets constantly collide and break-up into smaller ones. Yet, the droplet size distribution is rather narrow in comparison to the average droplet radius, as was observed in the internal combustion engines [20].

The fuel (*f*) and gas (*a*) concentrations C_f and C_a are related to the respective fuel and gas densities ρ_f and ρ_a via the relations:

$$C_f = \alpha\rho_f, \qquad C_a = (1-\alpha)\rho_a, \quad (6)$$

where α and (1 - α) are the corresponding volumetric fractions of fuel and ambient gas, respectively. We consider the region of the spray where α is sufficiently small so that the effect of droplets on the gas momentum transfer is negligible. In other words, the droplets are considered as passive tracers in the moving gas.

Droplets are assumed to experience only the drag force, and therefore their deceleration is expressed as:

$$\frac{d\mathbf{u}_d}{dt} = \frac{\mathbf{F}_d}{m_d} = -\frac{3}{8r_d}C_D\frac{\rho_a}{\rho_f}|\mathbf{u}_d - \mathbf{u}_a|(\mathbf{u}_d - \mathbf{u}_a) \quad (7)$$

where r_d is the droplet radius; $\mathbf{u}_d$ and $\mathbf{u}_a$ are the droplet and gas velocities, respectively; C_D is the drag coefficient, which dependence on the droplet Reynolds number is established empirically [21]:

$$\mathrm{Re} = \frac{2|\mathbf{u}_d - \mathbf{u}_a|\rho_a r_d}{\mu_a} \quad (8)$$

For Reynolds numbers smaller than 1 the drag coefficient is described by C_D = 24/Re. For Reynolds numbers above 1000 C_D = 0.44

During this process the droplets bring the surrounding gas into motion [22], [12]. After a short period of time (of the order of the droplets' relaxation time) the ambient gas' velocity and the fuel velocity equalize and the injection reaches a steady state. The time during which a steady state flow regime is achieved is related to the droplets characteristic relaxation time which for 30 μm drops is of the order of several hundreds of microseconds. Practically it is significantly shorter since the droplets break up during their motion, resulting in smaller droplets, having smaller relaxation time. Therefore, the relaxation time during which a typical droplet will accommodate

to the moving gas is small compared to the injection duration. Since fuel injection is an unsteady process, each droplet in the spray penetrates to a certain distance and accelerates the air around it. If we consider axial distances less than the spray penetration distance *S*, it may be safely assumed that the jet is at a steady state. This assumption also implies that in the laminar flow regime the gas-fuel relative velocity vanishes and therefore a single flow field may be considered:

$$\mathbf{u}_f = \mathbf{u}_a = \mathbf{u} \tag{9}$$

In internal combustion engines, movement of the piston and gas flow through valves in the combustion chamber cause movements in the ambient gas surrounding the jet. Also, in some combustion chambers, particularly in smaller engines, droplets may impinge the inner chamber walls. The present model is limited to the circumstances where the effect of this gas motion on the fuel injection is weak and the fuel jet effectively develops in a quiescent gas. Also, it is assumed that the combustion chamber to which fuel is injected is large enough or injection process is designed to prevent fuel droplets from reaching any walls.

Drops with sizes below one micron are involved in molecular Brownian motion, resulting from collisions with fast- moving gas molecules [21]. Such impingements instantaneously accelerate the droplet relative to the surrounding gas, thereby causing diffusive droplet flux, governed by the droplets Brownian Diffusivity *D*. Brownian motion and diffusive flux of drops with sizes exceeding one micron is rather weak and, in the absence of external forces, droplets closely follow the gas flow trajectory. On the other hand, in circumstances where the characteristic jet Reynolds number is rather high (about 10^4[23]) the jet flow becomes turbulent short distance after exiting the injection nozzle [19]. In such a situation turbulent gas motion combined with droplet inertia creates droplet-gas relative motion. The concomitant droplet turbulent flux is characterized by the corresponding turbulent diffusivity [24].

We first consider a laminar two-phase jet propagating in a gas having molecular viscosity $\boldsymbol{\nu}_a$. Then we use this solution in situation where the jet is turbulent upon replacement of $\boldsymbol{\nu}_a$ with the appropriate turbulent viscosity $\boldsymbol{\nu}_t$, in accordance with the solutions of Schlichting [24] and other studies [25].

Inlet Spray Properties

Fuel injection is a process which includes several physical phenomena, including fuel jet motion, its break-up, droplet formation and their propagation within the chamber. When the fuel jet leaves the nozzle hole, it is assumed to have a circular cross-section with a diameter proportional to the nozzle-hole radius r_i, and a uniform initial velocity u_i. The ratio between the cross-sectional areas of the jet and the nozzle is the coefficient of contraction C_c [10]. The initial velocity of the fuel jet is the product of the ideal velocity determined by the Bernoulli equation [26] and the coefficient of velocity of the nozzle C_v:

$$u_i = C_v\sqrt{2\Delta p / \rho_f} \tag{10}$$

By determining the inlet velocity of the fuel jet as in equation (10), the typical expressions for the inlet fuel mass flux and momentum flux are obtained:

$$\dot{m}_{fi} = C_c\pi r_i^2\rho_f u_i = \pi C_v C_c r_i^2\sqrt{2\rho_f\Delta p}$$

$$\dot{J}_i = C_c\pi r_i^2\rho_f u_i^2 = 2\pi C_v^2 C_c r_i^2\Delta p \tag{11}$$

Governing Equations

The flow of each phase (fuel and ambient gas) can be generally described by the laws of conservation of mass and momentum, each governing spatial and temporal evolution of fuel phase mass density and flow velocity.

The steady-state general equations of conservation is written in the approximation of a small volumetric fuel density $\alpha \ll 1$ and the ensuing condition (8), justifiable sufficiently far from the jet inlet. Namely we will use the following equations [27]:

1. Conservation of mass for the two phases:

$$\nabla\cdot\left(C_f\mathbf{u}\right) = D_f\nabla^2 C_f$$

$$\nabla\cdot\left(C_a\mathbf{u}\right) = D_a\nabla^2 C_a \tag{12}$$

   where D_f and $D_a = D_f = D$ are coefficients of diffusions of the binary fuel-air mixture.

2. The steady-state conservation of momentum for the two phases:

$$\nabla\cdot\left(C_a\mathbf{u}\mathbf{u}\right) = -\nabla p_a + \nabla\cdot\boldsymbol{\tau}_a + \mathbf{F}$$

$$\nabla\cdot\left(C_f\mathbf{u}\mathbf{u}\right) = -\mathbf{F} \tag{13}$$

In equation (13) p_a is the gas pressure, and **F** is the volumetric force density vector acting on the gas phase and stemming from the drag force acting on the droplets. The hydrodynamic Newtonian stress tensor $\boldsymbol{\tau}_a$ is characterized by an effective mixture viscosity μ, dependent on the fuel volume fraction [28]. In the dilute fuel volume fraction limit, the pressure and stress tensor induced by the fuel phase is neglected. Furthermore, by the same reason we set in equation (13) $1 - \alpha \approx 1$, **F** = 0, and neglect the dependency on α of all terms therein. Thus, the effective mixture viscosity μ is very close to the constant gas viscosity μ_a.

We also note that in view of (6) the sum of equations (12) yields the usual mass continuity equation for the whole mixture:

$$\nabla \cdot \mathbf{u} = 0$$

(14)

The above relation will be used in place of the second equation (12).

For circular nozzle geometry the jet is axially symmetric and the above equations (12), (13), (14) may be rewritten in the forms:

$$u_x \frac{\partial \alpha}{\partial x} + u_r \frac{\partial \alpha}{\partial r} = D\left[\frac{\partial^2 \alpha}{\partial x^2} + \frac{1}{r}\frac{\partial}{\partial r}\left(r\frac{\partial \alpha}{\partial r}\right)\right]$$

(15)

$$\frac{\partial}{\partial x}\left(\alpha u_x^{\,2}\right) + \frac{1}{r}\frac{\partial}{\partial r}\left(r\alpha u_x u_r\right) = 0$$

(16)

$$\frac{\partial}{\partial x}\left(u_x^{\,2}\right) + \frac{1}{r}\frac{\partial}{\partial r}\left(r u_x u_r\right) = -\frac{1}{\rho_a}\frac{\partial p}{\partial x} + \nu_a\left[\frac{\partial^2 u_x}{\partial x^2} + \frac{1}{r}\frac{\partial}{\partial r}\left(r\frac{\partial u_r}{\partial r}\right)\right]$$

(17)

$$\frac{\partial u_x}{\partial x} + \frac{1}{r}\frac{\partial (r u_r)}{\partial r} = 0$$

(18)

This system should generally be amended by the corresponding equation for the radial momentum components. However, as will be shown below it is unnecessary in view of the boundary layer nature of the jet assumed below.

For sufficiently long distances from the inlet, as expressed by the requirement that the characteristic jet Reynolds number greatly exceeds one, the radial jet width is significantly smaller than the corresponding axial distance from the inlet and also $u_x \gg u_r$ [24]. Therefore the radial momentum and mass conservation equations contain terms which are significantly smaller than those appearing in the axial transport equations. Furthermore, performing usual order of magnitude analysis in the axial transport equations, one obtains the equations of the two-phase jet in the following form:

$$u_x \frac{\partial \alpha}{\partial x} + u_r \frac{\partial \alpha}{\partial r} = \frac{D}{r}\frac{\partial}{\partial r}\left(r\frac{\partial \alpha}{\partial r}\right),$$

(19)

$$\frac{\partial}{\partial x}\left(r u_x^{\,2}\right) + \frac{\partial}{\partial r}\left(r u_x u_r\right) = \nu_a \frac{\partial}{\partial r}\left(r\frac{\partial u_x}{\partial r}\right),$$

(20)

to be considered jointly with (18). The boundary conditions for the above systems are:

$$r = 0: \;\; u_r = 0; \;\; \frac{\partial u_x}{\partial r} = 0; \;\; \frac{\partial \alpha}{\partial r} = 0$$

$$r \to \infty: \;\; u_x \to 0; \;\; \alpha \to 0$$

(21)

Solution for Steady State Two-Phase Laminar Jet

The governing equations (18), (20) were solved by Schlichting [24] for the single phase axisymmetric jet. A solution for the fuel volumetric fraction can then be obtained by using the equation of conservation of mass for the fuel phase (equation (19)).

Integrating the equation of conservation of mass for fuel (equation (19)) over the whole jet width and using conditions (21), we get:

$$2\pi \int_0^\infty \rho_f \alpha u_x r dr = \text{Const} = \dot{m}_{fi}$$

(22)

This means that the fuel mass flow in every cross-section of the spray is constant and equal to the fuel mass flux at the nozzle outlet, $\dot{m}_{fi}$.

Integrating the sum of the equations of conservation of momentum for the two phases jointly with (21) yields the condition of conservation of momentum flux in the axial direction, which is equal to the momentum flux at the nozzle outlet $\dot{J}_i$:

$$2\pi\rho_a \int_0^\infty u_x^{\,2} r dr + 2\pi\left(\rho_f - \rho_a\right)\int_0^\infty \alpha u_x^{\,2} r dr = \text{Const} = \dot{J}_i$$

(23)

In view of the smallness of the fuel volume fraction, the second integral term in equation (23) may be neglected. The requirement for a small volume fraction can thus be quantified as follows:

$$\alpha << \frac{\rho_a}{\rho_f - \rho_a}$$

(24)

Equations (18), (20) can be solved by defining a stream function Ψ similarly to the case of the single-phase laminar jet [24], where:

$$r u_x = \frac{\partial \Psi}{\partial r}, \quad r u_r = -\frac{\partial \Psi}{\partial x}$$

(25)

Similarly to the single phase jet, the stream function will be assumed to have the following functional form:

$$\Psi = \nu_a x F\left(\frac{r}{x}\right) = \nu_a x F\left(\eta\right),$$

(26)

where $\eta = r / x$ and F is a function to be determined. Substituting the velocity components into equation (20) with expressions derived from equations (25), (26), an ordinary differential equation for F is obtained:

$$\frac{FF'}{\eta^2} - \frac{F'^2}{\eta} - \frac{FF''}{\eta} = \frac{d}{d\eta}\left(F'' - \frac{F'}{\eta}\right)$$

(27)

The general solution of equation (27) which satisfies the necessary boundary conditions is [24]:

$$F = \frac{\xi^2}{1+\frac{1}{4}\xi^2}$$

(28)

where $\xi = \gamma\eta$ and γ is a constant to be determined below. Introducing this solution to equations (25), (26) allows obtaining an expression for the velocity components, similarly to the solution of Schlichting.

The solution for $F(\eta)$ is used to determine the fuel volume fraction α. Towards this goal assume α to be of the following functional form:

$$\alpha = \frac{1}{x} A\left(\xi\right)$$

(29)

The terms in equation (18) can be rewritten in terms of x, η, $F(\xi)$ and $A(\xi)$, resulting in an ordinary differential equation for $A(\xi)$:

$$-\left(A'F + F'A\right) = \frac{\partial}{\partial\xi}\left[\frac{D}{\nu}\xi A'\right]$$

(30)

The term D/ν is the fuel droplet phase Schmidt number Sc [21], which for micron size droplets is of order of thousand. Integration of this equation and applying the appropriate boundary conditions for $A(\xi)$, which can be derived from conditions (21), yields:

$$A(\xi) = \frac{C}{\left(1+\frac{1}{4}\xi^2\right)^{2Sc}}$$

(31)

wherein the constant C will be determined below. Using the expressions for F and $A(\xi)$ (equations (28), (31)) one can obtain analytical expressions for u_x, u_r, α:

$$u_x = \frac{\nu_a}{x}\frac{2\gamma^2}{\left(1+\frac{1}{4}\xi^2\right)^2}$$

(32)

$$u_r = \frac{\nu_a}{x}\gamma\left(\frac{\xi - \frac{1}{4}\xi^3}{\left(1+\frac{1}{4}\xi^2\right)^2}\right)$$

(33)

$$\alpha = \frac{C}{x\left(1+\frac{1}{4}\xi^2\right)^{2Sc}}$$

(34)

The constant γ can be found by substituting the expression (32) in the condition of constant momentum flux (23) to obtain:

$$\gamma = \sqrt{\frac{3\dot{J}_i}{16\pi {\nu_a}^2 \rho_a}}$$

(35)

The constant C can be found from the condition (22) of the fuel mass flow conservation:

$$C = \left(2Sc+1\right)\frac{\dot{m}_{fi}}{8\pi\rho_f\nu_a}$$

(36)

Extension to the Turbulent Jet

An analytical expression of the velocity field for single-phase turbulent jets was obtained by Schlichting [24], by solving the time averaged equations of conservation of mass and momentum. The equations are similar to the corresponding equations of conservation in laminar jets, except for the expression for the apparent turbulent shear stress which is assumed to be of the following form [24]:

$$\tau_t = \rho_a \nu_t \frac{\partial \overline{u_x}}{\partial r}, \tag{37}$$

where the over-bar refers to a time averaged value. Prandtl's mixing length assumption dictates that for boundary-layer turbulent flows the apparent turbulent viscosity is proportional to the radial gradient of the axial velocity:

$$\nu_t = l^2 \left| \frac{\partial \overline{u_x}}{\partial r} \right|, \tag{38}$$

where l is a certain length scale, known as Prandtl's mixing length, which is related to the characteristic size of turbulent eddies. A further simplification was proposed by Prandtl for flows far from solid boundaries, where the mixing length is assumed to be proportional to the width of the mixing zone b:

$$\left| \frac{\partial \overline{u_x}}{\partial r} \right| = \frac{\overline{u_{x max}} - \overline{u_{x \min}}}{b} \tag{39}$$

In jet flows [24], b is the width of the jet, the maximum velocity $\overline{u}_{x max}$ is obtained at the centerline and the minimum velocity has $\overline{u}_{x \min}$ a small value and can be neglected. Since the spray width is approximately proportional to x and the velocity is proportional to x^{-1} [24], the simplified turbulent viscosity remains constant and uniform. Then, a solution analogous to the laminar case is achieved. Schlichting proposed to use the proportionality of this term to $\sqrt{\dot{J}_i / \rho_a}$, derived from the boundary condition of conservation of mixture momentum flux (equation (23)). The turbulent viscosity may thus be rewritten in its final form:

$$\nu_t = C_t \sqrt{\dot{J}_i / \rho_a} \tag{40}$$

C_t is the coefficient of turbulent viscosity, which was determined experimentally in previous works. The different values for C_t were summarized in the paper of Abraham [22], and are presented in

Table 1. In the following sections, these values are used in the comparisons between the present model, existing empirical models and experimental results, and the value of C_t with which best agreement is achieved is found.

Table 1. Values of the turbulent viscosity coefficient C_t

Authors	C_t	Conditions
Schlichting	0.0161	-
Albertson et al.	0.0113	$x / r_i \geq 16$
Ricou and Spalding	0.0113	-
Hill	0.0113	$x / r_i \geq 26$
Crow and Champagne	0.0103	$x / r_i \geq 12$
Sforza and Mons	0.0099	$x / r_i \geq 20$
Taylor et al.	0.0092	$x / r_i \geq 20$

With constant turbulent viscosity, the time-averaged velocity components may be solved similarly to the laminar case, with the substitution of the molecular viscosity with the turbulent one and an appropriate substitution of the Schmidt number to the turbulent Schmidt number, defined as the ratio between the gas phase turbulent viscosity and the fuel turbulent diffusivity:

$$Sc \equiv \nu_t / D_t \tag{41}$$

Unlike the molecular Schmidt number, the value of the turbulent Schmidt number for micron-size particles is in the range 0.6 - 1 [29], [14].

Using equations (40), (41) and introducing the terms for mass and momentum flux from equation (11) the time averaged velocity components and fuel volume fraction α may be expressed in the final form:

$$\xi = \sqrt{\frac{3}{16\pi C_t^2}} \frac{r}{x}$$

$$\overline{u_x} = \sqrt{\frac{9 C_v^2 C_c}{32\pi C_t^2} \frac{\Delta p}{\rho_a}} \frac{r_i}{x} \frac{1}{\left(1 + \frac{1}{4}\xi^2\right)^2}$$

$$\overline{u_r} = \sqrt{\frac{3 C_v^2 C_c}{8} \frac{\Delta p}{\rho_a}} \frac{r_i}{x} \frac{\xi - \frac{1}{4}\xi^3}{\left(1 + \frac{1}{4}\xi^2\right)^2}$$

$$\overline{\alpha} = \frac{\sqrt{C_c}}{8 C_t \sqrt{\pi}} \sqrt{\frac{\rho_a}{\rho_f}} \frac{r_i}{x} \frac{(2Sc+1)}{\left(1 + \frac{1}{4}\xi^2\right)^{2Sc}} \tag{42}$$

RESULTS AND DISCUSSION

Analysis of the Model Results

Equations (42) describe the point-wise distribution of mixture velocity and fuel volume fraction in the spray. The fuel volume fraction distribution dictates that the fuel concentration gradually decreases with increasing radial distance from the spray axis of

symmetry. In the experimental works a spray boundary is often defined from which the spray dispersion angle is derived [10], [17]. It is noticeable that the value of the similarity variable ξ at the spray boundary, marked henceforth as ξ_b, is proportional to the tangent of the spray dispersion angle:

$$\xi_b = \sqrt{\frac{3}{16\pi C_t^2}}\left(\frac{r}{x}\right)_b = \sqrt{\frac{3}{16\pi C_t^2}}\tan\left(\frac{\theta}{2}\right) \tag{43}$$

In experimental works, where the fuel spray is measured by optical means [10], [17], the spray boundary may be optically determined with an accuracy limited by the light intensity in the spray image. Clearly, there is a degree of arbitrariness in the determination of the spray dispersion angle, for several reasons: First, the selection of the boundary light intensity may vary between different studies. Second, different imaging systems provide different images from which the spray dispersion angle is to be determined. Finally, the dispersion angle is measured at a certain distance from the nozzle, which also varies between different studies.

The equation of fuel volume fraction distribution in equation (42) yields a non-zero (however low) fuel concentration even very far from the nozzle due to the assumption of uniform turbulent viscosity. The spray dispersion angle may therefore be defined as a value of fuel volume fraction ε in which the spray boundary is determined. From this definition, the correlation for spray dispersion angles is as follows:

$$\tan\left(\frac{\theta}{2}\right) = 8C_t \times \sqrt{\frac{\pi}{3}\left[\left(\frac{\sqrt{C_c}}{8C_t\sqrt{\pi}}\sqrt{\frac{\rho_a}{\rho_f}}\frac{(2Sc+1)}{\varepsilon}\frac{r_i}{x}\right)^{1/2Sc} - 1\right]} \tag{44}$$

It can be seen that, in contrast to existing models, the spray dispersion angle in the present model varies with the axial distance from the injector nozzle, albeit the dependency is weak. This indicates that comparison between equation (44) to the experimental data collected for the spray dispersion angles in the experimental works is rather ambiguous. In contrast, as will be shown below, experimental validation of the radial distribution of fuel volume fraction in equation (42) can yield meaningful conclusions.

Another observation that can be made is that the spatial distributions of velocity and fuel volume fraction in equation (42) obey the relationships:

$$\overline{u_x}(x,\xi) = \overline{u_x}(x,0)\, f\left(\frac{\xi}{\xi_b}\right)$$

$$\overline{\alpha}(x,\xi) = \overline{\alpha}(x,0)\left(f\left(\frac{\xi}{\xi_b}\right)\right)^{Sc} \tag{45}$$

This is in accordance with several findings of experimental results [14].

Comparison with Experiments

Comparisons with available experimental data were performed for the model validation. We will first compare the general spray properties obtainable by averaging the local velocity and fuel volume fraction fields over the width of the spray, characterized by the value ξ_b at the spray boundary. For the latter we will use the experimental value of spray angle in order to avoid errors which are related to differences in the definition of spray boundary in various experimental studies.

The C_t values appearing in Table 1 were analyzed using the least-square method, namely minimizing a discrepancy between the results of calculation and the experimental data of [10, 14, 17, 18]. It was found that $C_t = 0.0113$ allows best agreement with overall experimental results.

It should be noted that even though the model is limited to dilute regions of the spray, the experimental data for regions close to the injection nozzle were not omitted in order to provide a broader perspective of the comparisons.

Spray Penetration

The Spray penetration $S(t)$ is received by averaging the axial velocity over the spray cross-section. We will use the relation $\overline{u}_{x\,mean} = \frac{dS}{dt}$ where $S = x$ is the axial distance from the nozzle or, by definition, the spray penetration. Using also the initial condition $S(0) = 0$ the following equation is obtained:

$$\frac{dS}{dt} = \overline{u}_{x\,mean} = \frac{\int_0^b \overline{u_x} r dr}{\int_0^b r dr} \tag{46}$$

The expression for axial velocity in equation (42) is introduced into equation (46) to obtain the spray penetration over time:

$$S(t) = \frac{8}{\tan\left(\frac{\theta}{2}\right)}\left(\frac{\pi C_t^2 C_v^2 C_c}{8}\right)^{0.25} \times \sqrt{1-\left(1+\frac{3}{64\pi C_t^2}\tan^2\left(\frac{\theta}{2}\right)\right)^{-1}}\left(\frac{\Delta p}{\rho_a}\right)^{0.25}\sqrt{2r_i t} \tag{47}$$

It should be noted that equation (47) accords with the form of semi-empirical models of spray penetration (equation (3)).

Results from the experiments of Naber & Siebers for spray penetration [10] have been compared with the model of Hiroyasu & Arai [9] (equation (2)) and equation (47) for sprays

in different ambient densities. This comparison is shown in Figures 2, 3, 4, 5. The experimental conditions are summarized in Table 2.

Table 2. Experimental conditions in the measurements of spray penetration

$\rho_f \ [kg/m^3]$	705
$r_i \ [mm]$	0. 1285
$\Delta p \ [MPa]$	137
C_c	0.81
C_v	0.765

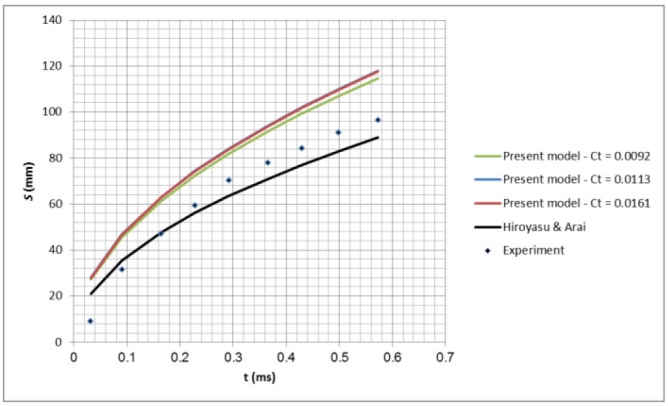

Figure 2. Comparison of penetration vs. time. Ambient Density 3.6 kg/m^3

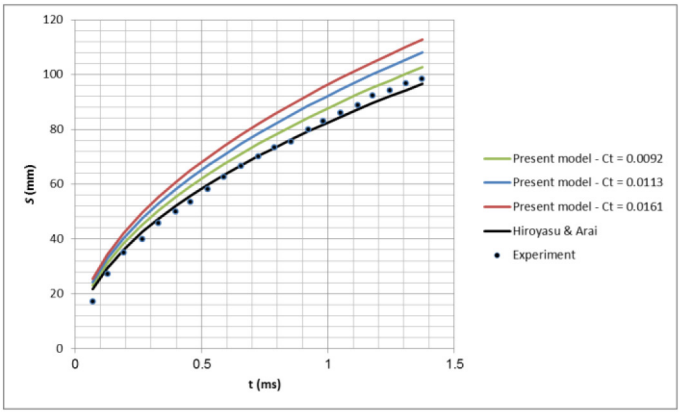

Figure 3. Comparison of penetration vs. time. Ambient Density 14.8 kg/m^3

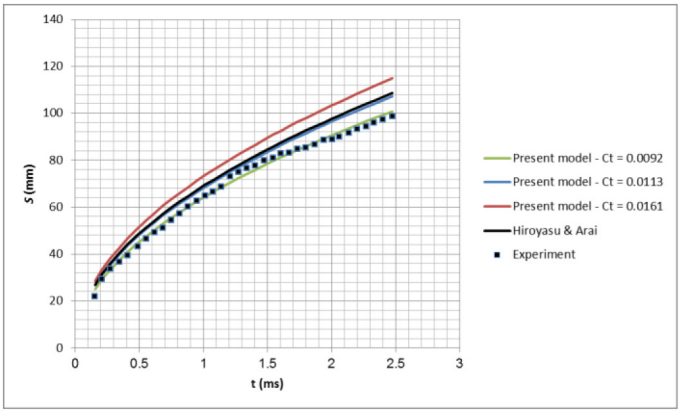

Figure 4. Comparison of penetration vs. time. Ambient Density 30.2 kg/m^3

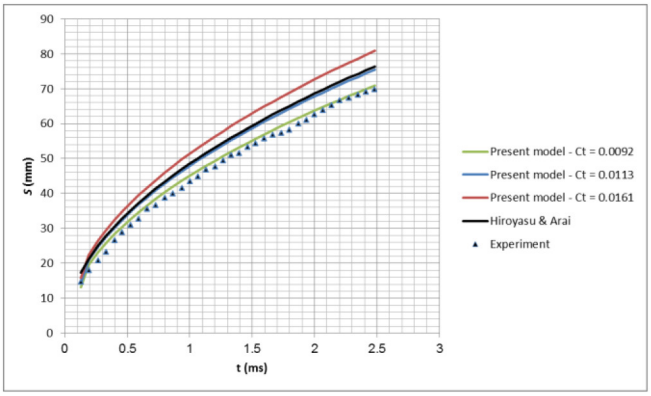

Figure 5. Comparison of penetration vs. time. Ambient Density 124 kg/m^3

As can be seen in Figures 2, 3, 4, 5, a good agreement exists between the predictions of the present model and the experimental data for high ambient densities. As previously mentioned, the value of 0.0113 was chosen for the coefficient of turbulent viscosity C_t in the following comparisons because it was found to best agree with overall experimental results. For lower densities (Figure 2), the disagreement between the present model and experimental data becomes noticeable. This trend may be related to the influence of the ambient density on the spray motion, expressed in the condition of dilution (equation (24)). This condition for fuel volume fraction can be easily linked to a dilution distance, which is the distance from the nozzle from which the condition of dilution is satisfied, through the solution for the fuel volume fraction expressed in equation (42):

$$x >> (2Sc+1)\frac{\sqrt{C_c}}{8C_t\sqrt{\pi}}\frac{\rho_f-\rho_a}{\sqrt{\rho_f\rho_a}}r_i \equiv x_{dilution} \tag{48}$$

This condition implies that, in low ambient densities, the condition (24) is not satisfied in the relevant region of the spray. It should be noticed that ambient densities in internal combustion engines are usually much higher than the discussed density [20].

Cross-Sectional Averaged Fuel Concentration

The cross-sectional averaged fuel concentration can be found by averaging the local fuel concentration over the width of the spray:

$$\overline{C_f} = \frac{\pi\int_0^{\xi_b}\overline{\alpha}\rho_f\xi d\xi}{\pi\int_0^{\xi_b}\xi d\xi} = \frac{16\sqrt{C_c}C_t\sqrt{\rho_a\rho_f}}{3\sqrt{\pi}\tan^2\left(\frac{\theta}{2}\right)}\frac{1+2Sc}{1-2Sc}\frac{r_i}{x}\times \left(\left(1+\frac{3}{64C_t^2}\tan^2\left(\frac{\theta}{2}\right)\right)^{1-2Sc}-1\right) \tag{49}$$

Results from the experiments of Kamimoto et al. [17] for cross-sectional averaged fuel concentration are compared here with the model of Wakuri et al [11] (equation (4)) and equation (49) for two sprays. Experimental conditions for both sprays were summarized in Table 3. An upper and lower boundary for the Schmidt number of 1 and 0.7 were taken. Results from the comparison are displayed in Figures 6, 7.

Table 3. Experimental conditions of the spray study in [17] used for the comparison of the cross-sectional averaged fuel concentration with the present model

	Spray A	**Spray B**
r_i $[mm]$	0.07	0.1
$\dot{m}_{fi}$ [g/s]	2.46	4.56
Δp $[MPa]$	21.295	17.796
ρ_a $[kg/m^3]$	17.3	17.3
T [K]	300	300
ν_a $[\mu Pa \cdot s]$	18.12	18.12
Nozzle coefficients	$C_D = C_c = 0.821$	$C_D = C_c = 0.8$ (typically used values [10])
$\tan(\theta/2)$	0.19	0.2
Injection time [ms]	3.05	2.5

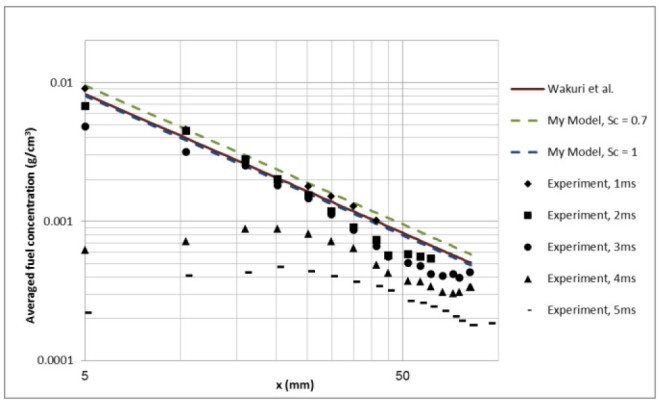

Figure 6. Comparison of cross-sectional averaged fuel concentration vs. axial distance from the nozzle, Spray A

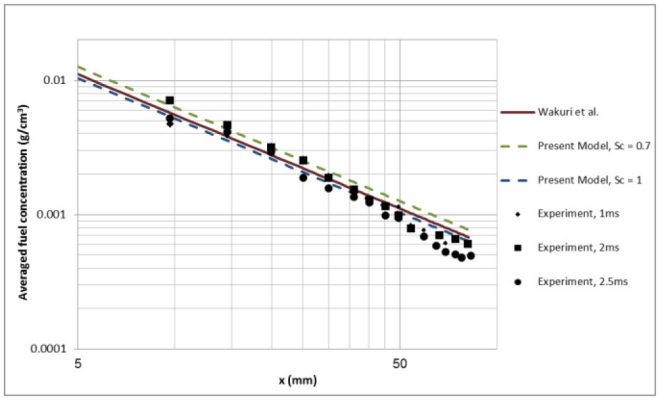

Figure 7. Comparison of cross-sectional averaged fuel concentration vs. axial distance from the nozzle, Spray B

It can be seen that a good agreement between the present model and the experimental results is achieved for Schmidt numbers varying between 0.7 and 1, and the model provides satisfactory predictions even close to the injection nozzle, where the condition of dilution is not met. Results of experiments in spray *A* show that after the nozzle closes and fuel is no longer injected to the chamber, the fuel spray behavior changes and the fuel concentration in the region closer to the nozzle begins to decrease. The present model relies on the assumption of constant injection of fuel into the cylinder, and so predictions of spray properties are limited to the stages of injection in which the injector is still open.

Radial Velocity Distribution

The radial distribution of axial velocity in equation (42) in various axial distances from the nozzle was compared against the experimental work presented in the paper of Desantes et al. [14], and the Gaussian approximation of the one-dimensional model presented in their paper. The experimental conditions are listed in Table 4. The experiments were conducted under non-evaporative conditions and an engine-like ambient density.

Table 4. Experimental conditions of the spray study in [14]

ρ_a $[kg/m^3]$	40
r_i $[mm]$	0.073
Δp $[MPa]$	150
u_i $[m/s]$	238

It can be seen in the results of the comparisons, presented in Figures 8, 9, 10, 11, 12, 13, that good agreement was found between experimental work and the present model. It may also be seen that results obtained from the Gaussian approximation in the model of Desantes et al. [14] are very close in values to results obtained from the present model. This is despite the fact that the one-dimensional model relies on either measured or correlated values of the spray dispersion angle, while the present model does not require the spray dispersion angle to provide similar predictions.

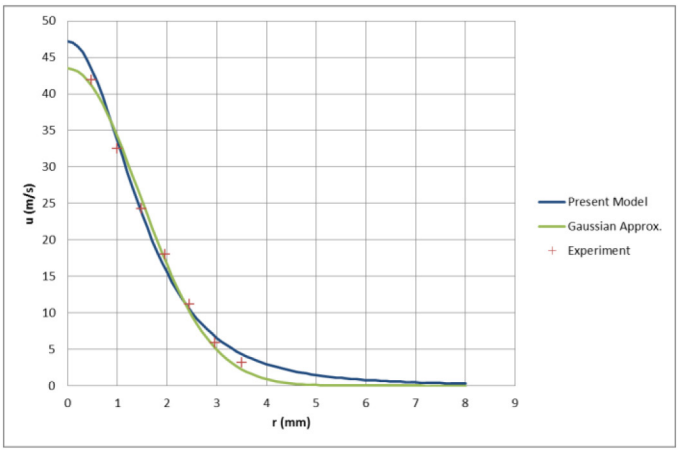

Figure 8. Comparison of radial distribution of axial velocity at 25 mm from the nozzle

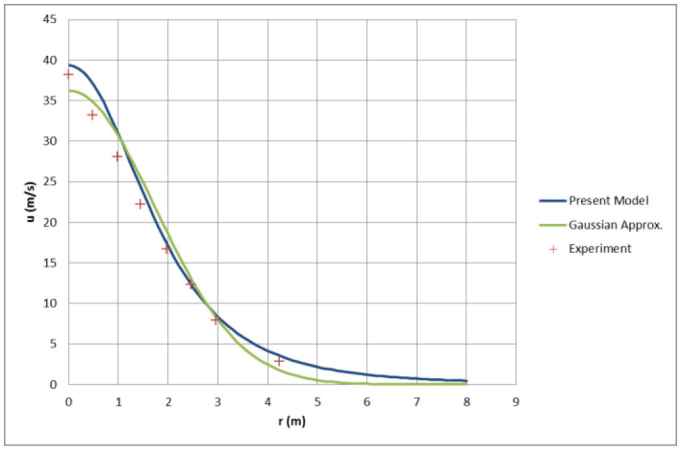

Figure 9. Comparison of radial distribution of axial velocity at 30 mm from the nozzle

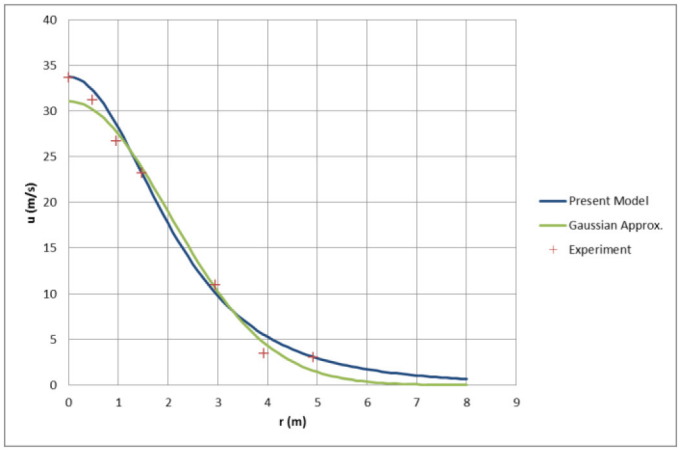

Figure 10. Comparison of radial distribution of axial velocity at 35 mm from the nozzle

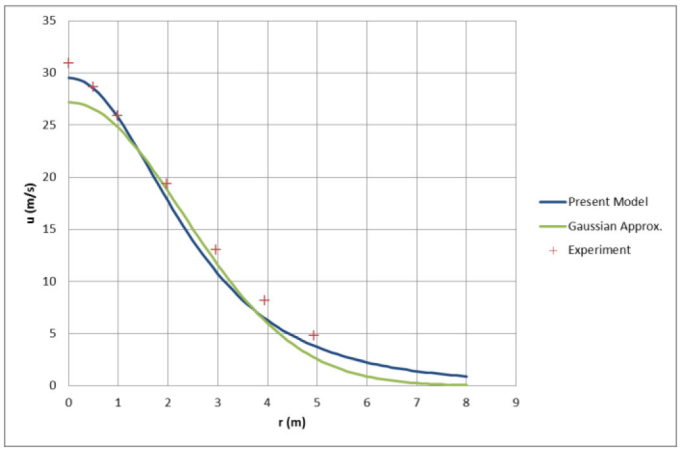

Figure 11. Comparison of radial distribution of axial velocity at 40 mm from the nozzle

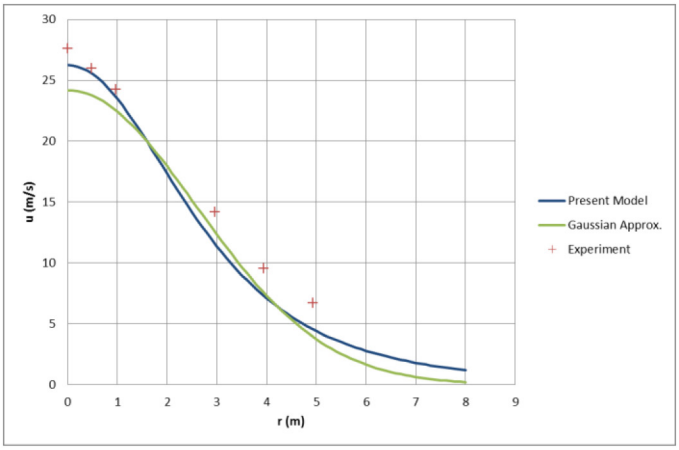

Figure 12. Comparison of radial distribution of axial velocity at 45 mm from the nozzle

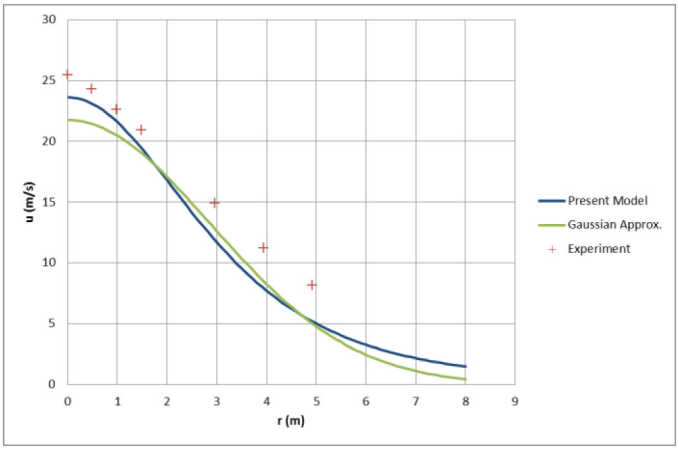

Figure 13. Comparison of radial distribution of axial velocity at 50 mm from the nozzle

It should be noted that the measured value of momentum flux from the nozzle presented in the latter paper does not agree with results of the Gaussian approximation and results in an unrealistic inlet injection conditions. The momentum was therefore fixed to be in accordance with the Gaussian profile of the one-dimensional model.

Radial Fuel Volume Fraction Distribution

Comparisons of fuel volume fraction distribution between the present model (equation (42)) and the experimental results presented in the work of Payri et al. [18] are presented here. Two properties were examined in the comparison; the first is the centerline fuel volume fraction as a function of the axial distance from the nozzle, and the second is the radial distribution of the fuel volume fraction at a certain distance from the nozzle. Both properties were examined for three ambient gas densities and, in some cases, compared also to the one-dimensional model presented in the paper of Payri et al. [18]. The experimental conditions are listed in Table 5. The chosen value of the Schmidt number is 0.8. The comparisons are displayed in Figures 14, 15, 16, 17, 18, 19.

Table 5. Experimental conditions of the spray study in [18]

r_i $[mm]$	0.045
Δp $[MPa]$	150
T $[K]$	300
$\dot{m}_{fi}$ [g/s]	2.63
$\dot{J}_i$ $[N]$	1.54

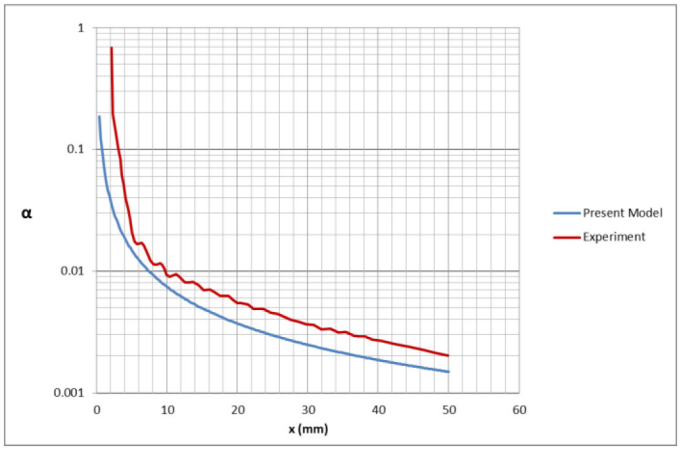

Figure 14. Comparison of the centerline fuel volume fraction vs axial distance from the nozzle. Ambient density: 7.6 kg/m^3

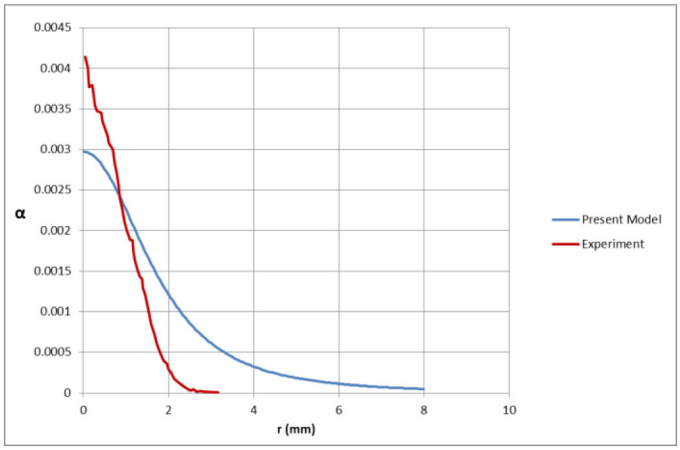

Figure 15. Comparison of radial distribution of the fuel volume fraction. Ambient density: 7.6 kg/m^3

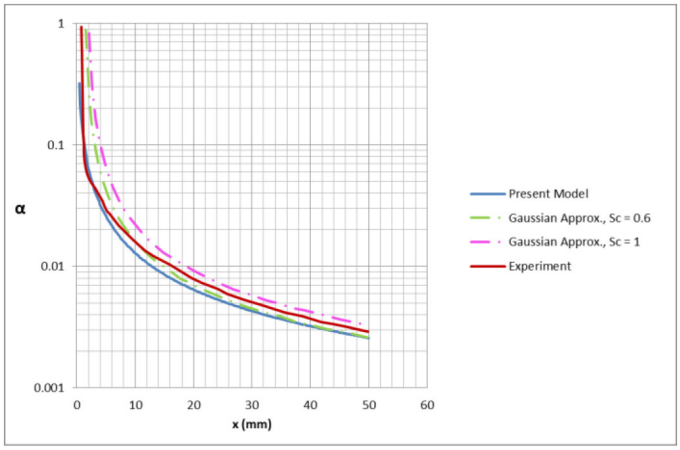

Figure 16. Comparison of centerline fuel volume fraction versus axial distance from the nozzle. Ambient density: 22.8 kg/m^3

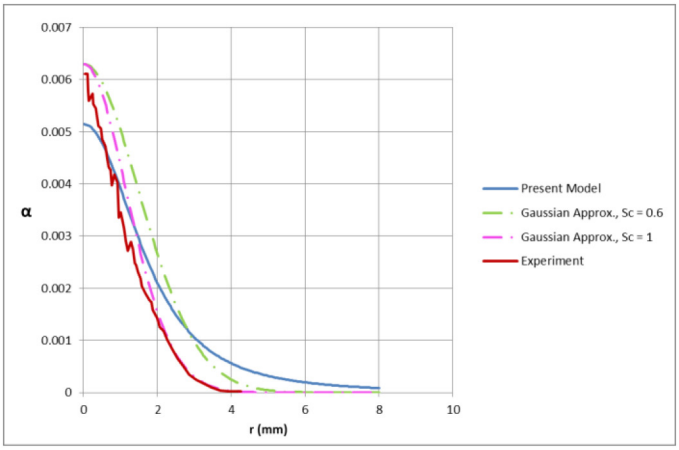

Figure 17. Comparison of radial distribution of fuel volume fraction. Ambient density: 22.8 kg/m^3

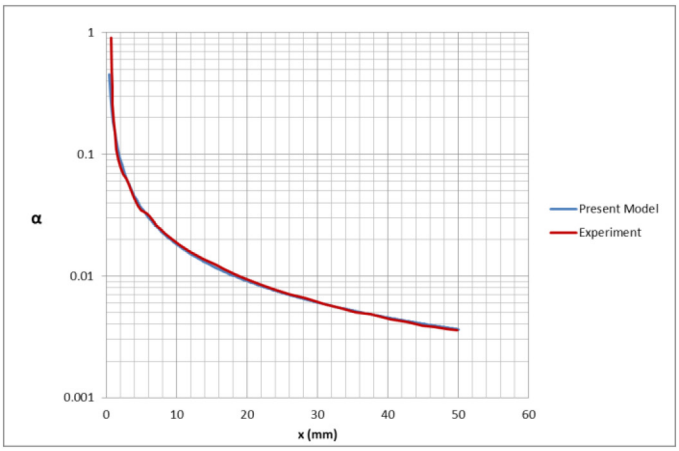

Figure 18. Comparison of centerline fuel volume fraction versus axial distance from the nozzle. Ambient density: 45.6 kg/m^3

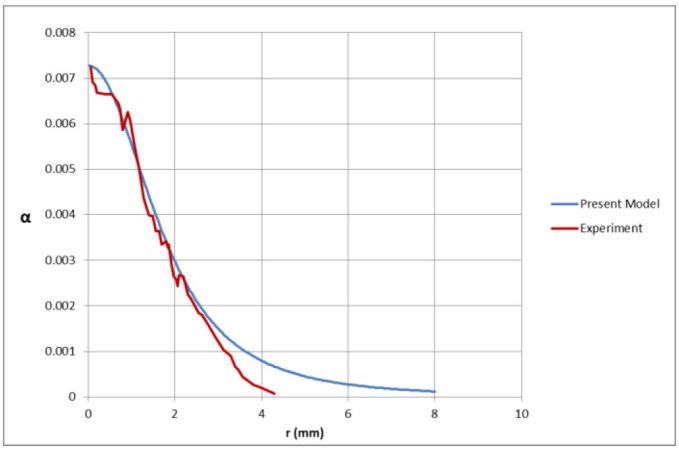

Figure 19. Comparison of radial distribution of fuel volume fraction. Ambient density: 45.6 kg/m^3

It can be shown that for engine-like ambient densities (usually higher than 22 kg/m^3) an acceptable agreement with experimental results with the present model is achieved. In these comparisons a good agreement between the model and experimental results can also be observed near the nozzle, where the fuel volume fraction approaches unity (suggesting a liquid fuel jet), where the model assumptions are invalid due to

the inapplicability of the condition of dilution. There are, however, discrepancies between the present model and experimental results for low ambient densities. These discrepancies, which were also observed for spray penetration, apparently result from the inapplicability of the assumptions of dilute fuel phase, as mentioned previously. For higher ambient densities, a good agreement can be seen between the present model and experimental results. The main difference between the two may be found along the spray boundary. Experimental results show rapid decay in fuel volume fraction for larger radial distances. In contrast, the present model predicts a wide radial distribution of fuel. For an ambient density of 45.6 kg/m^3, this difference leads to an error of about 0.1 percent in fuel concentration (assuming constant fuel density of 720 kg/m^3). However, as there exists a difficulty in measuring spray concentration in the region of the spray boundary [18], the error could also stem from the measurement inaccuracy. Another discrepancy is found in comparisons of centerline fuel volume fraction very close to the nozzle. This discrepancy could, again, be a consequence of the relatively higher fuel concentration in the spray close to the nozzle.

For the ambient gas density of 22.8 kg/m^3, the Gaussian approximation for radial fuel volume fraction distribution of the one-dimensional model which also accords with the experimental data. However, the Gaussian approximation can only be determined if the spray angle is measured or determined from an empirical correlation. In contrast, the present model does not require this *a priori* information.

CONCLUSIONS

In this work, an analytical two-dimensional model was developed for calculation of fuel local concentration in an axisymmetric dilute spray. This model was implemented to a turbulent fuel spray in conditions typical for internal combustion engines. The model predictions were compared with the existing correlations and the available experimental data. A good agreement with experimental results was found in all comparisons with ambient density higher than 14.8 kg/m^3.

The advantage of the present model over available existing models is its ability to calculate both axial and radial distributions of spray properties such as fuel concentration and velocity without reliance on any measured or correlated spray properties. An accurate prediction of the local fuel concentration in a spray greatly improves the model's ability to predict engine characteristics such as pollutant formation, local temperatures in the combustion chamber and many more. It should be mentioned that the present model does not require extensive calculations or computational resources. This enables incorporation of the present spray model in existing engine models, and can be used for analysis of engine performance as well as optimization of design and operation parameters such as the nozzle geometry, injection timing, fuel pressure etc. Furthermore, the ability of the present model to obtain predictions without prior measurements or empirical correlations allows the use of this model without any need of calibration to the predicted spray. This is important for optimizations of injection parameters without the need of extensive model verifications.

It is important to note that the model was developed under several assumptions, such as dilute fuel phase, steady state injection and quiescent combustion chamber. These assumptions limit the applicability of the model. For more general situations such as those prevailing in several unsteady injection systems at a complex flow regime the model should be generalized to a wider range of operating conditions.

REFERENCES

1. Baumgarten C., “Mixture Formation in Internal Combustion Engines,” Springer; 2006.
2. Abani N., Munnannur A. and Reitz RD., “Reduction of Numerical Parameter Dependencies in Diesel Spray Models,” Journal of Engineering for Gas Turbines and Power. 2008;130.
3. Iyer V. and Abraham J., “Penetration and Dispersion of Transient Gas Jets and Sprays,” Combustion Science and Technology. 1997:315-334.
4. Jung, D. and Assanis, D., “Multi-Zone DI Diesel Spray Combustion Model for Cycle Simulation Studies of Engine Performance and Emissions,” SAE Technical Paper 2001-01-1246, 2001, doi:10.4271/2001-01-1246.
5. Pastor J.V., López J.J., García J.M., Pastor J.M., “A 1D Model for the Description of Mixing-Controlled Inert Diesel Sprays,” Fuel 87. 2008:2871-2885.
6. Morel T. and Wahiduzzaman S., “Modeling of Diesel Combustion and Emissions,” XXVI FISITA Congress. 1996.
7. Sazhin S.S., Feng G. and Heikal M.R., “A model for fuel spray penetration,” Fuel. 2001;80(15):2171-2180.
8. Schweitzer P.H., “Penetration of Oil Sprays,” Journal of Applied Physics. 1938 December;9(12):735-741.
9. Hiroyasu H. and Arai M., “Fuel Spray Penetration and Spray Angle in Diesel Engines,” Transactions of JSME. 1980;21:5-11.
10. Naber, J. and Siebers, D., “Effects of Gas Density and Vaporization on Penetration and Dispersion of Diesel Sprays,” SAE Technical Paper 960034, 1996, doi:10.4271/960034.
11. Wakuri Y., Fujii M., Amitani T. and Tsuneya R., “Studies of the Penetration of Fuel Spray in a Diesel Engine,” Bulletin of JSME. 1960;3:123-130.
12. Ghosh S. and Hunt J.C.R., “Induced Air Velocity within Droplet Driven Sprays,” Proceedings of the Royal Society. 1994 105-127.
13. Dent, J., “A Basis for the Comparison of Various Experimental Methods for Studying Spray Penetration,” SAE Technical Paper 710571, 1971, doi:10.4271/710571.
14. Desantes J.M., Payri R., Garcia J.M. and Salvador F.J., “A Contribution to the Understanding of Isothermal Diesel Spray Dynamics,” Fuel 86. 2007:1093-1101.
15. Ranz W.E., “Some Experiments on Orifice Sprays,” Canadian J. Chem. Eng. 1958;36:175.
16. Reitz, R. and Bracco, F., “On the Dependence of Spray Angle and Other Spray Parameters on Nozzle Design and Operating Conditions,” SAE Technical Paper 790494, 1979, doi:10.4271/790494.
17. Kamimoto, T., Ahn, S., Chang, Y., Kobayashi, H. et al., “Measurement of Droplet Diameter and Fuel Concentration in a Non-Evaporating Diesel Spray by Means of an Image Analysis of Shadow Photographs,” SAE Technical Paper 840276, 1984, doi:10.4271/840276.
18. Payri R., Gimeno J., Martí P. and Manin J., “Fuel Concentration in Isothermal Diesel Sprays through Structured Planar Laser,” International Journal of Heat and Fluid Flow 34. 2012:98-106.
19. Lin S.P. and Reitz R.D., “Drop and Spray Formation From a Liquid Jet,” Annual Review of Fluid Mechanics. 1998;30:85-105.
20. Heywood J.B., “Internal Combustion Engine Fundamentals,” McGraw Hill; 1988.
21. Hinds W.C., “Aerosol Technology: Properties, Behavior and Measurements of Airborne Particles,” John Wiley & sons; 1999.

22. Abraham J., “Entrainment Characteristics of Transien Gas Jets,” Numerical Heat Transfer, Part A: Applications. 1996;30(4):347-364.
23. Dimotakis P.E., “The Mixing Transition in Turbulent Flows,” Journal of Fluid Mechanics. 2000;409:69-98.
24. Schlichting H., “Boundary Layer Theory,” 7th ed. McGraw Hill; 1955.
25. Melville W.K. and Bray K.N.C., “A Model fo theTwo-Phase Turbulent Jet,” International Journal of Heat and Mass Transfer 1979:647-656.
26. Fox R.W., McDonald A.T. and Pritchard P.J., “Introduction to Fluid Dynamics,” 6th ed. John Wiley & Sons; 2004.
27. Bird R.B., Stewart W.E. and Lightfoot E.N., “Transport Phenomena,” 2nd ed. John Wiley & Sons; 2002.
28. Gidaspow D., “Multiphase Flow and Fluidization: Continuum and Kinetic Theory Descriptions,” 1st ed. Harcourt Brace & Sons; 1994.
29. Polezhaev Y.V., Korshunov A.V. and Gabbasova G.V., “Turbulence and Turbulent Viscosity in Jet Flows,” Heat and Mass Transfer and Physical Gas Dynamics. 2007 378-382.